

The nuclear rim protein Amo1 is required for proper microtubule cytoskeleton organisation in fission yeast

Mercedes Pardo^{1,*‡} and Paul Nurse²

¹Cell Cycle Laboratory, Cancer Research UK, 44 Lincoln's Inn Fields, London, WC2A 3PX, UK

²The Rockefeller University, 1230 York Avenue, New York, NY 10021, USA

*Present address: Proteomic Mass Spectrometry, The Wellcome Trust Sanger Institute, Wellcome Trust Genome Campus, Hinxton, Cambridge, CB10 1SA, UK

‡Corresponding author (e-mail: mp3@sanger.ac.uk)

Accepted 3 February 2005

Journal of Cell Science 118, 1705-1714 Published by The Company of Biologists 2005
doi:10.1242/jcs.02305

Summary

Microtubules have a central role in cell division and cell polarity in eukaryotic cells. The fission yeast is a useful organism for studying microtubule regulation owing to the highly organised nature of its microtubular arrays. To better understand microtubule dynamics and organisation we carried out a screen that identified over 30 genes whose overexpression resulted in microtubule cytoskeleton abnormalities. Here we describe a novel nucleoporin-like protein, Amo1, identified in this screen. Amo1 localises to the nuclear rim in a punctate pattern that does not overlap with nuclear pore complex components. *Amo1Δ* cells are bent, and they have fewer microtubule bundles that curl

around the cell ends. The microtubules in *amo1Δ* cells have longer dwelling times at the cell tips, and grow in an uncoordinated fashion. Lack of Amo1 also causes a polarity defect. Amo1 is not required for the microtubule loading of several factors affecting microtubule dynamics, and does not seem to be required for nuclear pore function.

Supplementary material available online at
<http://jcs.biologists.org/cgi/content/full/118/8/1705/DC1>

Key words: Microtubules, Fission yeast, Nuclear pore complex

Introduction

The microtubule cytoskeleton carries out essential functions in eukaryotic cells. It is responsible for chromosome segregation, contributes to cleavage during cell division, and also participates in the maintenance of cell shape and polarity. The fission yeast *Schizosaccharomyces pombe* is an excellent model system for studying mechanisms regulating the microtubule cytoskeleton. Interphase microtubules in *S. pombe* are organised in two to five bundles longitudinal to the long axis of the cell (Hagan, 1998). These bundles are composed of several microtubules with an antiparallel configuration, with their plus ends pointing towards the cell tips and the minus ends overlapping in a medial region of the cell in the vicinity of the nucleus (Drummond and Cross, 2000; Tran et al., 2001; Sagolla et al., 2003). The microtubule cytoskeleton is very dynamic; microtubules generally grow from the cell centre until they reach the cell ends where they stop growing and undergo catastrophe. The cell end marker protein Tea1 is transported by microtubules and deposited at cell ends, where it associates with other polarity factors to regulate cell polarity (Behrens and Nurse, 2002; Snaith and Sawin, 2003; Feierbach et al., 2004). Several proteins have been described that modulate microtubule stability and length, leading to a model in which Tip1 complexed with the kinesin Tea2 on microtubules regulates microtubule catastrophe such that it occurs at cell tips, thereby ensuring proper microtubule organisation (Brunner and Nurse, 2000; Busch et al., 2004). Microtubules contact the nuclear membrane and contribute to nuclear positioning in the cell middle by pushing forces

produced as microtubules polymerise against the cell tips (Tran et al., 2001). The nature of the attachment between microtubules and nuclear envelope and the molecules involved are, however, not yet known. When microtubules are depolymerised they shrink back to between one and three tubulin stubs at the nuclear periphery, termed iMTOCs, from where microtubules repolymerise upon microtubule regrowth. Components of the γ -TURC (γ -tubulin ring complex) localise at these iMTOCs, together with Mod20/Mbo1, a centrosomin-related protein that seems to recruit them to these sites (Sawin et al., 2004; Venkatram et al., 2004). The molecular composition of iMTOCs is not known, and it is still unclear whether they nucleate microtubules themselves or stabilise nascent microtubules.

To gain insight into the machinery that organises the microtubule cytoskeleton during interphase we performed an overexpression screen and identified over 30 genes which, when overexpressed, lead to an abnormal microtubule cytoskeleton. Here we describe the characterisation of Amo1, a novel fission yeast protein identified in this screen, which is required for correct termination of microtubule growth at cell ends in interphase. Amo1 has moderate sequence similarity to nucleoporins, and localises to the nuclear rim, suggesting that the interplay between microtubules and nucleus is important for the regulation of microtubule dynamics.

Materials and Methods

Yeast strains

Strains used in this study are listed in Table 1. Cells were grown in

Table 1. Yeast strains used in this study

Strain	Relevant genotype	Source
MP155	pSV40- <i>GFP-atb2::LEU2 leu1-32</i>	This study
MP164	pSV40- <i>GFP-atb2::LEU2 ura4-D18</i>	This study
MP294	<i>amo1Δ::kanMX6</i>	This study
MP335	<i>amo1Δ::kanMX6 pSV40-GFP-atb2::LEU2</i>	This study
MP339	<i>amo1-GFP::kanMX6</i>	This study
MP370	<i>amo1Δ::kanMX6 tea2-GFP::kanMX6</i>	This study
MP373	<i>amo1-13myc::kanMX6</i>	This study
MP378	<i>amo1Δ::kanMX6 alp16-GFP::kanMX6</i>	This study
MP402	<i>tea1Δ::ura4+ amo1Δ::kanMX6</i>	This study
MP417	<i>amo1Δ::kanMX6 NLS-LacI-GFP</i>	This study
MP421	<i>amo1Δ::kanMX6 klp5-PK-GFP::ura4+</i>	This study
MP443	<i>amo1Δ::kanMX6 alp4-GFP::kanMX6</i>	This study
MP458	<i>amo1Δ::kanMX6 tip1-GFP::kanMX6</i>	This study
MP466	<i>cut11-GFP::ura4+ nmt1-GFP-atb2::lys1+</i>	This study
MP467	<i>amo1Δ::kanMX6 cut11-GFP::ura4+ nmt1-GFP-atb2::lys1+</i>	This study
MP468	<i>amo1Δ::kanMX6 mod20-GFP::kanMX6</i>	This study
MP470	pSV40- <i>GFP-atb2::LEU2 amo1-mRFP1::kanMX6</i>	This study
MP7b	NLS-LacI-GFP	A. Decottignies*
MS593	<i>alp4-GFP::kanMX6</i>	T. Toda [‡]
PN1734	<i>tea1Δ::ura4+</i>	Lab collection
PN2432	<i>tea2-GFP::kanMX6</i>	Lab collection
PN3643	<i>tip1-GFP::kanMX6</i>	Lab collection
PN4575	<i>alp16-GFP::kanMX6</i>	T. Toda [‡]
PN4581	<i>klp5-PK-GFP::ura4+</i>	R. West [§]
PN4752	<i>mod20-GFP::kanMX6</i>	K. Sawin [¶]
PN68	Wild type	Lab collection

*Université Catholique de Louvain, Belgium.
[‡]Cancer Research UK, London, UK.
[§]University of Colorado, Boulder, CO.
[¶]Wellcome Trust Centre for Cell Biology, Edinburgh, UK.

Edinburgh minimal medium (EMM) supplemented with amino acids and 0.2 μM thiamine if required or YES (yeast extract with supplements) media at 32°C (unless otherwise stated). Strains were constructed by standard genetic means (Moreno et al., 1991). Gene deletions were performed by PCR-mediated gene replacement as previously described (Bahler et al., 1998). *Amo1* was tagged with GFP, mRFP1 (Campbell et al., 2002) or 13myc at the C-terminus by the same method. G418-resistant clones were screened by colony PCR for integration at the correct locus. The tagged-*Amo1* strains behaved as wild-type cells in all conditions tested.

Screening for defective microtubules

A fission yeast strain constitutively expressing green fluorescent protein (GFP)-tagged α -tubulin was constructed as follows: *GFP-atb2* was amplified by PCR from pDQ105 (Ding et al., 1998) and cloned behind the SV40 promoter in pSM-1 (Russell, 1989). The resulting plasmid pMP102 was stably integrated into strain PN22 (h *leu1-32*) to produce strain MP155. MP155 was then crossed to a *ura4-D18* strain to generate MP164.

Eight mini-normalised cDNA libraries were constructed by pooling equal amounts of 800 individual clones from a *S. pombe* cDNA library placed under the control of the *nmt1* promoter. The library represented transcripts from exponential growth, shmooing and meiosis (2:1:1). Each pool was transformed in MP164 and 300 transformants per pool were picked and arrayed in selective master plates containing thiamine to repress expression of the cDNAs. Transformants were inoculated in 96-well plates containing selective medium without thiamine and incubated at 32°C for 16 hours. Transformants were then transferred to glass-bottomed 96-well plates coated with lectin and incubated a further 2–4 hours at 32°C. These plates were screened visually for abnormalities in the microtubule cytoskeleton using a Zeiss Axioplan fluorescence microscope.

Immunofluorescence and microscopy

Cells were fixed in -70°C methanol for tubulin and Tea1 immunofluorescence, 10% TCA at 4°C for Tea3 and with 4% formaldehyde in PEM buffer for nuclear pore complex immunofluorescence, and were processed according to standard methods. Tubulin was visualised using TAT-1 monoclonal antibody provided by Dr Gull (University of Manchester, UK). Tea1 was detected with affinity-purified Tea1 antibody (Mata and Nurse, 1997). Tea3 was detected with Tea3 antibody (Arellano et al., 2002). Nup189 antibody (Tange et al., 2002) was a kind gift from Dr Niwa (Kaznsa DNA Research Institute, Kisatazu, Japan). Sad1 antibody (Hagan and Yanagida, 1995) was a kind gift from Dr Hagan. Anti-myc 9E10 antibody was used for detection of *Amo1-myc*. Alexa 488 and Alexa 546 antibodies were from Molecular Probes. To visualise actin, cells were fixed in 4% formaldehyde and stained with Rhodamine-Phalloidin (Molecular Probes). Chromosomal DNA was stained with DAPI. Imaging was carried out with a Zeiss LSM 510 laser-scanning confocal microscope or an Olympus wide-field inverted microscope.

Images were generated by deconvolution wide-field fluorescence microscopy using the Olympus wide-field inverted microscope. Images were collected and processed with DeltaVision image acquisition software (Applied Precision). Time-lapse series for microtubule dynamics and nuclear envelope deformations were acquired using the same Olympus inverted microscope, either in a single focal plane or in multiple focal planes at 0.4 μm steps. Kymograph construction of interphase microtubules was done as described previously (Sagolla et al., 2003), except that microtubule bundles were filmed in a single focal plane. Microtubule dynamics values given in the text are mean±s.d.

Physiological experiments

Microtubules were depolymerised by treating cells with 25 μg/ml of carbendazim (MBC) for 10 minutes or chilling cultures in ice-cold water for 30 minutes. For microtubule regrowth experiments, MBC was washed out by filtration and cells resuspended in fresh medium, or flasks were transferred from the cold water to shaking water baths at 25 or 32°C. Samples were fixed as described above. Time-lapse imaging of cells for growth pattern experiments was performed as previously described (Niccoli et al., 2003). Latrunculin A (Molecular Probes) pulse experiments were performed as previously described (Niccoli et al., 2003). For re-feeding experiments cells were grown in YES at 32°C for 30 hours and diluted 1:25 in fresh medium. Branching was scored after 3 hours.

Results

Screening for genes regulating the microtubule cytoskeleton

To identify novel genes regulating the microtubule cytoskeleton in fission yeast we carried out an overexpression screen using a *S. pombe nmt1* promoter-based cDNA library made using transcripts from cells in exponential vegetative growth, shmooing and meiosis. Eight hundred individual clones from this library were pooled in groups of 100 to make eight normalised mini-libraries that were transformed into a fission yeast strain constitutively expressing GFP-tagged α -tubulin (see Materials and Methods). This strain has normal-looking microtubules and allows full induction of cDNA expression upon thiamine removal without affecting GFP-tubulin levels. Three hundred individual transformants per mini-library were arrayed in master plates containing thiamine to allow screening in triplicate. Cells were then transferred to 96-well plates, incubated in minimal medium lacking thiamine

for 18–20 hours, and screened visually using a fluorescence microscope for microtubule defects.

After screening a total of 800 cDNAs, corresponding to 722 ORFs, we isolated 39 different clones that reproducibly caused microtubule defects when overexpressed (supplementary material, Table S1). Each clone was isolated one to three times, indicating that we had screened each mini-library thoroughly although not to saturation. Six of these clones had previously been identified and characterised as involved in microtubule or mitotic function. The rest were novel or not previously reported to function in microtubule organisation. The identified genes could be grouped in several functional categories: microtubule-associated (5), vesicle trafficking (3), signalling (7), chaperones (4), ubiquitin-related (3), metabolism (6), nuclear functions (5) and orphans (6).

To test if the identified genes had a direct effect on microtubule organisation and/or dynamics, we deleted the 33 non-microtubule related genes (supplementary material, Table S1). Twenty-eight haploid deleted strains were viable and were further assayed for growth and morphology at different temperatures and sensitivity to the microtubule-depolymerising drugs MBC and thiabendazole (TBZ). We also examined their microtubules by immunofluorescence. Two of the viable haploid strains deleted for novel genes showed altered growth and morphology, differential sensitivity to microtubule-depolymerising drugs, and aberrant microtubule organisation. Here we present work on one of these genes, SPBC15D4.10c, named *amo1* for ‘aberrant microtubules’ when overexpressed (see Fig. 1A).

The remaining five deletions caused lethality; one of them was defective in spore germination, whereas the rest formed microcolonies of one to 100 cells. Examination of these cells

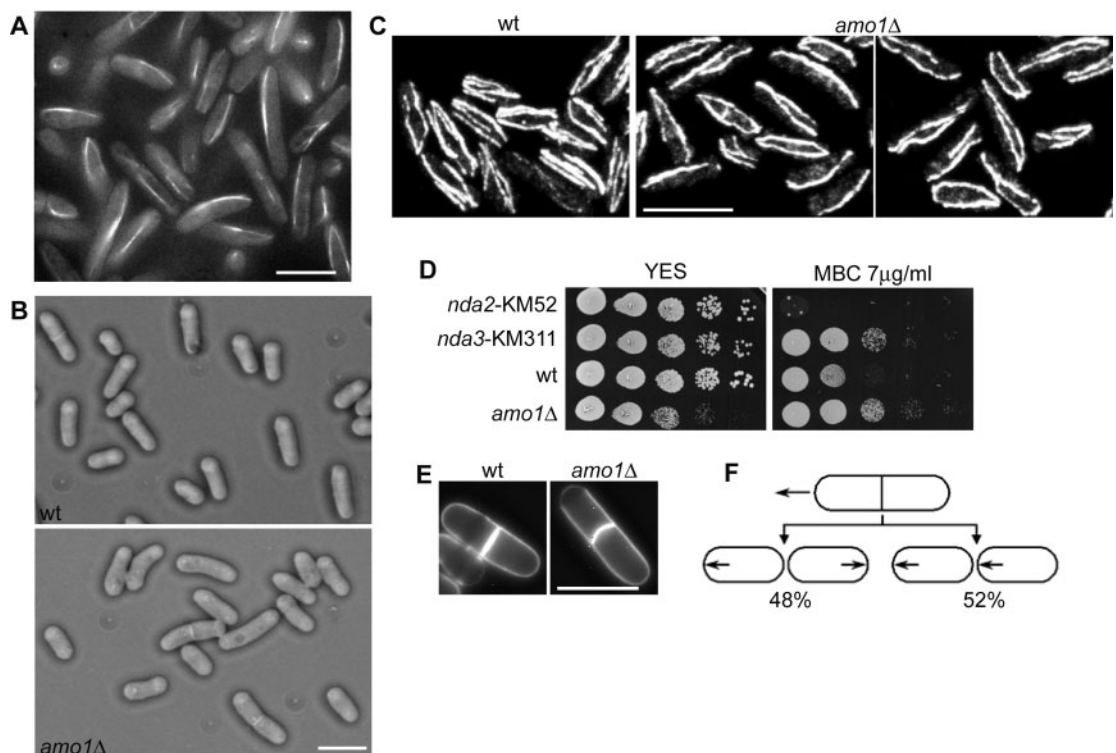
by tubulin immunofluorescence did not reveal any obvious microtubular defects.

Amo1Δ cells have altered microtubule cytoskeleton and polarity

Tetrad analysis of the heterozygous deleted diploid revealed that *amo1Δ* cells grew slower than wild-type cells. We therefore examined growth at different temperatures. *Amo1Δ* haploid cells grew slower than the wild type at 18, 25, 32 and 36°C. In addition, we observed that 8% of exponentially growing cells at 32°C were bent or curved (Fig. 1B). Branch formation in bent cells can be enhanced upon re-growth from stationary phase (Browning et al., 2000), so we grew *amo1Δ* cells to stationary phase, and then re-fed and incubated them for 3 hours, after which we scored branching. Although 75% of control *tea1Δ* cells were branched, *amo1Δ* cells did not branch.

We examined microtubule organisation by immunofluorescence. In wild-type cells there are usually 2–5 bundles of microtubules per cell (3.44 ± 0.85 , $n=158$ cells; values are mean \pm s.d.), parallel to the long axis. In contrast, *amo1Δ* cells had fewer microtubule bundles (2.25 ± 0.82 , $n=304$ cells). These bundles were sometimes thicker, and curved around the cell tips in 30% of cells (Fig. 1C). This phenotype was similar to the *amo1* overexpression phenotype, which basically consisted of a single thick microtubule bundle on one side of the cell (Fig. 1A). As nuclear positioning is dependent on microtubules (Tran et al., 2001) we examined the position of the nucleus in *amo1Δ* cells. Wild-type fission yeast cells maintained the nucleus in the middle of the cell, but the nucleus was off centre in 20% of *amo1Δ* cells. As expected, septum

Fig. 1. A role for Amo1 in microtubule organisation and polarity. (A) Overexpression of *amo1* leads to bundling of microtubules on one side of the cell. (B) Differential interference contrast microscopy images of wild-type cells (wt) and *amo1Δ* cells from plates. (C) Tubulin immunofluorescence of wild-type and *amo1Δ* cells. (D) MBC sensitivity spot assay. Cells from indicated strains were grown to mid-exponential phase, and tenfold serial dilutions spotted on plates containing the indicated amount of MBC. (E) Calcofluor White staining of septated wild-type and *amo1Δ* cells. (F) Growth patterns of pairs of cells after cell division were monitored.



The two patterns observed are shown, with percentages of total cells scored. Bar, 10 μ m.

positioning was also slightly offset in 15% of septating *amo1Δ* cells.

Differential sensitivities to microtubule depolymerising drugs are often indicative of a defective mitotic spindle checkpoint or abnormal microtubule behaviour. We carried out sensitivity tests to the microtubule drugs MBC and TBZ by spot dilution assays, and found that *amo1Δ* cells were resistant to MBC, at levels comparable to those of the *nda3-KM311* mutant (Fig. 1D). *Amo1Δ* cells were also resistant to TBZ (data not shown). Asynchronously growing populations of *amo1Δ* cells had a low mitotic index (5% of *amo1Δ* cells have spindles, compared to 10% of wild-type cells), which probably accounts for the slow growth. However, we observed no evidence of chromosome segregation defects or spindle abnormalities in these cells. Overexpression of Amo1 caused chromosome mis-segregation (data not shown), but this could be due to indirect as well as direct effects.

After cell division, fission yeast cells start growing from one end, and when they reach a critical size they switch growth to the new end and become bipolar, a transition called NETO (new end take-off) (Mitchison and Nurse, 1985). We observed that *amo1Δ* cells grew mainly from one end, with 80% of cells being monopolar compared to 35% monopolar cells in the wild type (Fig. 1E). This suggests that *amo1Δ* cells have a NETO defect. We then monitored cell growth after cell division and scored growth patterns in live *amo1Δ* cells. Time-lapse imaging of *amo1Δ* dividing cells showed that daughter cells that inherited a growing end used it as a site for growth. However, cells that did not inherit a growing end resumed growth randomly from either the new end (52%), that is, the one formed after septation, or from the old non-growing end (48%, Fig. 1F). It has been shown that an increase in the pool of free monomeric actin is sufficient to cause a switch from monopolar to bipolar actin in fission yeast cells, provided that both cell ends are marked as potential sites of growth (Rupes et al., 1999). To test if *amo1Δ* cells were able to recognise both cell ends as such, we depolymerised actin with latrunculin A (Lat A) and then removed the drug allowing actin to repolymerise. After the Lat A pulse, 50% of *amo1Δ* cells became bipolar compared with 20% before drug treatment (data not shown), suggesting that the NETO defect is not due to lack of recognition of the new end, but rather is a result of an inability to perform the switch and activate growth at the new end. These results indicate that *amo1Δ* cells have abnormal interphase microtubules and are defective in cell polarity.

Amo1 localises at the nuclear periphery

We next examined the intracellular localisation of Amo1. The endogenous *amo1* gene was tagged with GFP at the C-terminus, and the fusion protein was judged to be functional based on normal growth, morphology and sensitivity to MBC. In living cells, Amo1-GFP protein expressed from the endogenous promoter was localised to the nuclear rim in all stages of the cell cycle (Fig. 2A,B). It showed a punctate pattern, reminiscent of nuclear pore proteins (Chen et al., 2004), which lacked enrichment in any particular region of the nucleus. In mitosis, Amo1-GFP could be observed at the nuclear membrane, revealing the typical shoe-shape nucleus of an early anaphase cell, and the thread of nuclear envelope that

remains between the two separating nuclei in late anaphase (Fig. 2A, arrowheads). Immunofluorescence staining of Amo1-myc with anti-myc antibodies showed the same pattern of localisation (Fig. 2C; see also Fig. 5B). Amo1-myc did not colocalise with Sad1 (Hagan and Yanagida, 1995), suggesting that Amo1 is not localised at the spindle pole body (Fig. 2C).

To test if microtubules were required for this localisation we depolymerised microtubules with MBC and looked at the localisation of Amo1-GFP in live cells after 5, 30 and 60 minutes. Even after 60 minutes of MBC treatment Amo1 remained around the nucleus (Fig. 2D), indicating that its localisation is not dependent on microtubules.

We also tested if the Amo1 dots colocalised with the microtubule stubs that remain after microtubule depolymerisation with MBC. Cells expressing GFP-tubulin and Amo1-mRFP1 (monomeric red fluorescent protein) (Campbell et al., 2002) were treated with MBC for 10 minutes and then imaged in several focal sections spanning the whole cell, using the FITC and TRITC filters sequentially. We did not detect any colocalisation of Amo1-mRFP1 with the microtubule stubs, neither the most intense and largest one that probably corresponds to the SPB, nor the smaller and fainter ones (Fig. 2E), indicating that Amo1 is not localised at MTOCs.

Microtubule dynamics in *amo1Δ* cells

As interphase MTOCs are distributed mainly around the nuclear periphery, we examined whether *amo1* plays a role in microtubule nucleation by carrying out microtubule depolymerisation and regrowth experiments. After 10 minutes of MBC treatment microtubules were depolymerised to tubulin stubs or dots in essentially all wild-type cells (Fig. 3A). In contrast, polymerised microtubules remained in 30% of MBC-treated *amo1Δ* cells, suggesting that microtubules are more stable than in wild-type cells. One minute after washing out the MBC, microtubules had repolymerised in 93% of wild-type cells. *Amo1Δ* cells were equally efficient in microtubule repolymerisation, with 96% of cells having repolymerised microtubules after a 1-minute incubation in fresh medium. Microtubule bundling and curling could already be observed in *amo1Δ* cells at this stage and was more pronounced after 2 minutes (data not shown). We observed similar behaviour in cold-treated cells. Cold treatment for 30 minutes completely depolymerised microtubules in essentially all wild-type and *amo1Δ* cells (Fig. 3A). One minute after the shift to 32°C, short microtubules had repolymerised in over 90% of both wild-type and *amo1Δ* cells, and 2 minutes later, microtubules appeared normal in almost all cells. These results show that Amo1 does not appear to be required for microtubule nucleation or polymerisation.

We next investigated the attachment of microtubules to the nuclear envelope by filming live cells expressing GFP-tubulin and Cut11-GFP, a nuclear envelope marker (West et al., 1998). In wild-type cells we observed nuclear envelope deformations that correlated with, and are likely to be caused by microtubules pushing on the cell tip in the opposite direction to the deformation (supplementary material, Movie 1) (Tran et al., 2001). *Amo1Δ* cells also showed nuclear membrane deformations as microtubule bundles grew against the cell tips (supplementary material, Movie 2), suggesting that microtubules in *amo1Δ* cells can attach to the nuclear envelope.

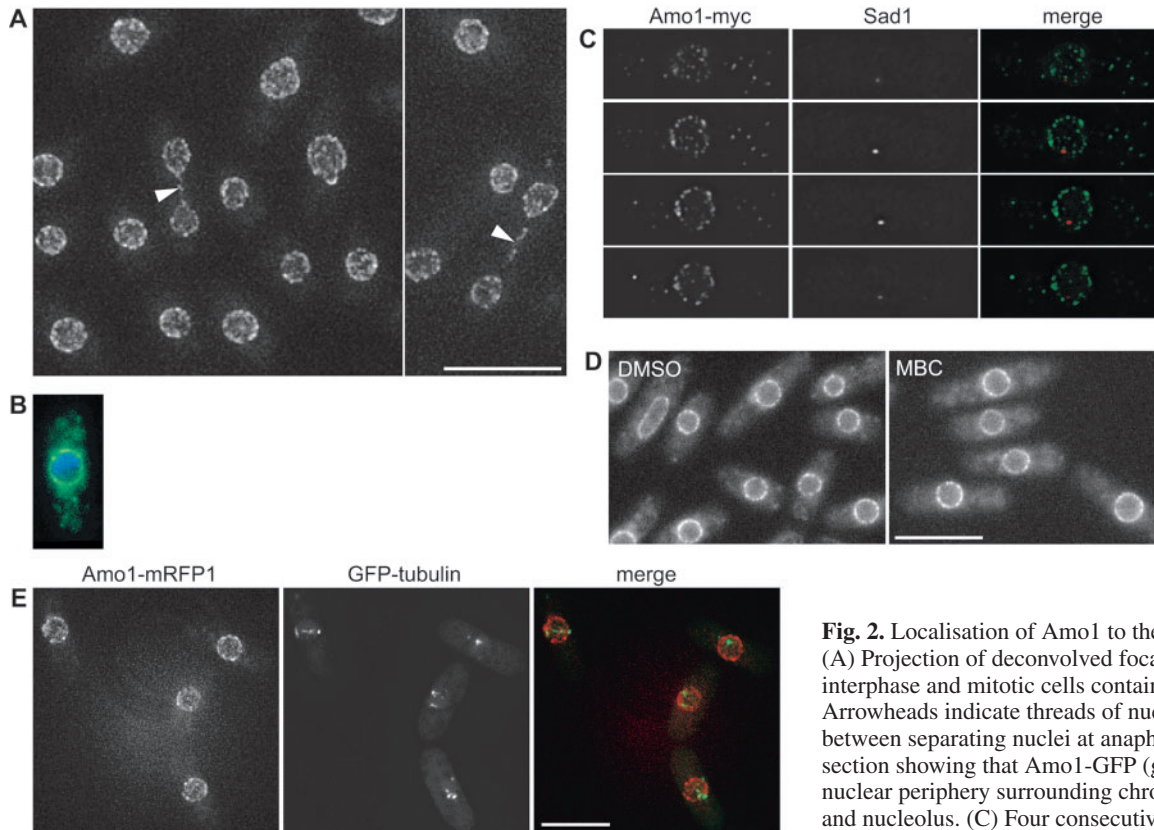


Fig. 2. Localisation of Amo1 to the nuclear surface. (A) Projection of deconvolved focal sections of live interphase and mitotic cells containing Amo1-GFP. Arrowheads indicate threads of nuclear membrane between separating nuclei at anaphase. (B) Single focal section showing that Amo1-GFP (green) localises to the nuclear periphery surrounding chromosomal DNA (blue) and nucleolus. (C) Four consecutive deconvolved focal sections showing Amo1-myc (green) and Sad1 (red)

detected by immunofluorescence. (D) Amo1-GFP localisation in control (DMSO) and MBC-treated cells. (E). Deconvolved projection showing live MBC-treated cells expressing GFP-tubulin (green) and Amo1-mRFP1 (red). Bar, 10 μm .

To gain further insight into the microtubular phenotype, we analysed microtubule dynamics in live *amo1* Δ cells. Kymographs were used to analyse the dynamics of microtubules, as they allow individual microtubules in the bundle to be monitored (Sagolla et al., 2003). We filmed wild-type and *amo1* Δ cells expressing GFP-tubulin in a single plane, focusing on a single microtubule bundle, and then constructed kymographs of these bundles. Polymerisation and depolymerisation rates were calculated from the slopes of the triangles described by individual microtubules as described before (Sagolla et al., 2003). Wild-type microtubules grew with a speed of 2.34 ± 0.43 $\mu\text{m}/\text{minute}$ ($n=31$ MTs) and microtubules from *amo1* Δ cells polymerised with a speed of 2.29 ± 0.67 $\mu\text{m}/\text{minute}$ ($n=26$ MTs). The depolymerisation speed of shrinking microtubules was 23.39 ± 10.25 $\mu\text{m}/\text{minute}$ ($n=31$ MTs) in the wild type and 23.77 ± 8.45 $\mu\text{m}/\text{minute}$ ($n=31$ MTs) in *amo1* Δ cells. We therefore conclude that there are no significant differences in the microtubule growth or shrinkage speeds between wild-type and *amo1* Δ cells.

We next determined the dwelling time of microtubules at cell ends. Whole cells were filmed by imaging several focal planes across the entire thickness of the cell, and we measured how long microtubules contacted the cell cortex at the cell end before undergoing depolymerisation. We found that the dwelling time of microtubule bundles at the cell tip was 58.8 ± 41.9 seconds ($n=39$ MTs, 9 cells) in wild-type cells and 96.7 ± 59.3 seconds ($n=42$ MTs, 16 cells) in *amo1* Δ . To assess if this difference was significant we performed a Student's *t*-test. The probability of

this difference occurring randomly is $P < 0.001$, suggesting that the difference is significant. Whilst analysing these films we observed that in *amo1* Δ cells more than one microtubule in a bundle often contacted the cell tip at the same time. We therefore measured dwelling times of individual microtubules contacting the cell tip and determined these to be 58.1 ± 23.5 seconds ($n=20$ MTs) in the wild type and 77.0 ± 30.4 seconds ($n=17$ MTs) in *amo1* Δ cells. The probability calculated by the Student's *t*-test is $P < 0.04$. Thus there is an increase in the dwelling time of bundled and individual microtubules at cell tips in *amo1* Δ cells.

It has been recently reported that interphase microtubules encounter the cell tip one at a time, with one microtubule in a bundle not reaching the tip until the previous one has already begun to depolymerise (Sagolla et al., 2003) (Fig. 3B, arrowheads; supplementary material Fig. S1). By careful examination of films and kymographs we observed that in *amo1* Δ cells there were often two or three microtubules in the same bundle touching the cell tip at the same time (Fig. 3C, arrowheads). After a while they usually depolymerised sequentially (supplementary material Fig. S1), although in some cases we noticed two microtubules depolymerising together. We scored for bundles with two or more microtubules touching the cell tip simultaneously in whole cell films and determined that these occurred with a frequency of 0.144 bundles per minute in wild-type cells (18 cells, 90 minutes' filming time). This phenomenon was more frequent in *amo1* Δ cells, occurring at a rate of 0.488 bundles per minute with more than one microtubule touching the tip (25 cells, 125 minutes' filming time). We believe

that this accounts for the longer dwelling time of microtubule bundles at cell tips we measured in *amo1Δ* cells. The extended time for which microtubules dwell at cell tips may be responsible

for the microtubule curling round the cell ends as it is more probable that both ends of the bundle will be touching and pushing against the cell tip at the same time. As a control, we scored other events, such as microtubule separation/fragmentation (where a microtubule bundle breaks up, or two microtubules in one bundle become detached), and microtubule fusion/bundling (two microtubules joining into one bundle). These occurred at similar frequency in wild-type and mutant cells: we observed 0.077 microtubule fragmentations per minute in the wild type and 0.088 per minute in *amo1Δ* cells, and 0.177 fusing/bundling microtubules per minute in the wild type and 0.12 fusing/bundling microtubules per minute in *amo1Δ* cells.

Localisation of the cell end marker Tea1 relies on microtubule transport to the cell ends and deposition at the cortex as the microtubule depolymerises (Behrens and Nurse, 2002). We analysed the localisation of Tea1 in *amo1Δ* cells by immunostaining with affinity-purified antibodies (Fig. 3D). In both wild-type and *amo1Δ* cells Tea1 was observed as dots on microtubules, suggesting that loading of this factor onto microtubules was not affected in cells lacking *amo1*. Tea1 was also found to be at cell tips in the majority of *amo1Δ* cells, but there were several abnormalities in its localisation. We observed that 89% of wild-type cells had free Tea1 (not associated with a microtubule end) at both cell ends and 11% of cells had free Tea1 only at one tip. In contrast, 73% of *amo1Δ* cells had free Tea1 on both cell ends, 22% had Tea1 not associated with microtubules in one end, and 4.5% did not have any Tea1 at cell tips not associated with microtubules. In addition, we observed abnormal accumulation of Tea1 in the lateral cortex of some cells (Fig. 3D, arrowhead). This suggests that the abnormal microtubule behaviour affects Tea1 localisation at cell ends.

We next constructed a double mutant *tea1Δ amo1Δ*. Exponentially growing *tea1Δ* cells are generally bent; some branch after shift to high temperature (20%) (Mata and Nurse, 1997) or re-feeding from stationary phase (75%). In contrast, 10% of

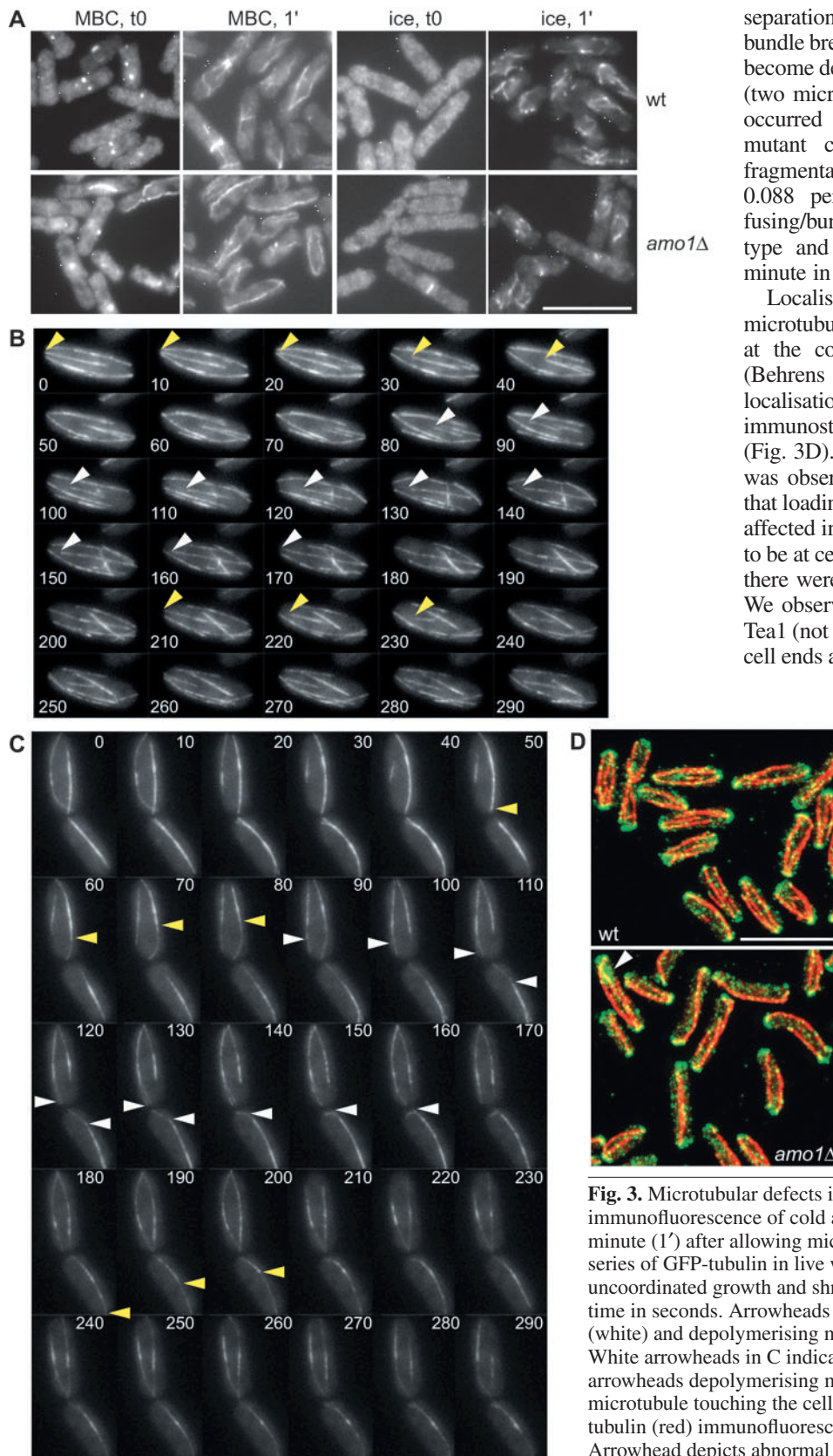


Fig. 3. Microtubular defects in *amo1Δ* cells. (A) Tubulin immunofluorescence of cold and MBC treated cells at time 0 (t0) and 1 minute (1') after allowing microtubule repolymerisation. (B,C) Time-lapse series of GFP-tubulin in live wild-type (B) and *amo1Δ* cells (C) showing uncoordinated growth and shrinkage in *amo1Δ* cells. Numbers indicate time in seconds. Arrowheads in B indicate polymerising microtubules (white) and depolymerising microtubules (yellow) in the same bundle. White arrowheads in C indicate polymerising microtubules and yellow arrowheads depolymerising microtubules in bundles with more than one microtubule touching the cell tip at the same time. (D) Tea1 (green) and tubulin (red) immunofluorescence in wild-type and *amo1Δ* cells. Arrowhead depicts abnormal accumulation of Tea1. Bar, 10 μ m.

exponentially growing *tea1Δ amo1Δ* cells formed branches, in conditions when no *tea1Δ* or *amo1Δ* cells did. Similar results were obtained with a variety of *tea1* ts mutants (data not shown). This suggests that Tea1 and Amo1 cooperate in the maintenance of cell polarity.

Given the localisation of Amo1 on the nuclear periphery, the potential site of microtubule loading of several proteins (Behrens and Nurse, 2002; Browning et al., 2003; Busch et al., 2004), we asked if Amo1 was required for the loading on microtubules of other factors affecting microtubule dynamics. Klp5 is a kinesin required for maintaining the normal length of microtubules in interphase (West et al., 2001). In its absence microtubules are abnormally long and curl around cell ends. Klp5-GFP was properly localised on microtubules in interphase *amo1Δ* cells (Fig. 4), and on spindles during mitosis in *amo1Δ* cells (data not shown). Another kinesin, Tea2, was observed as dots on microtubules and at cell ends in *amo1Δ* cells, similar to wild-type cells (Fig. 4). Tip1, the fission yeast CLIP-170-like protein, localises to dots on microtubules and to the cell ends (Brunner and Nurse, 2000). We found that Tip1-GFP localised to streaming cytoplasmic dots and to the cell ends in the majority of cells, similar to that observed in the wild type (Fig. 4). Even though Tip1-GFP was present in both cell ends in most *amo1Δ* cells, it seemed to form a less extended cap at the cell end than in wild-type cells, and was often found as few discrete dots. The difference was, however, very subtle. The γ -tubulin complex protein Alp4 is localised in multiple small dots ('satellites') on microtubules in addition to the spindle pole body (SPB) localisation (Zimmerman et al., 2004). Lack of γ -tubulin complex proteins also leads to microtubule defects similar to those described for *amo1Δ* cells. Therefore we explored the localisation of γ -tubulin complex components. Localisation of Alp4-GFP at both the SPB and the satellites was unaffected in *amo1Δ* cells (Fig. 4), and Alp16-GFP was also properly localised at the SPB and equatorial microtubule organising centres (EMTOCs) (data not shown). Mod20/Mbo1 is a centrosomin-related protein required for microtubule nucleation, that colocalises with the γ -tubulin complex at the SPB, EMTOCs and microtubule satellites (Sawin et al., 2004; Venkatram et al., 2004). Mod20-GFP was also properly localised to MTOCs and microtubules in *amo1Δ* cells (Fig. 4). These results indicate that Amo1 is not required for loading of these factors on microtubules.

Amo1 is not required for nucleo-cytoplasmic transport

When BLAST searches were performed with Amo1, nucleoporins from several organisms showed similarities with this protein. *Saccharomyces cerevisiae* Nup42 was the closest homologue, and the similarity was mainly based on the presence of FG (Phe-Gly) repeats (Fig. 5A), which are characteristic of the family of FG nucleoporins (Strawn et al., 2004). To determine if Amo1 is a component of nuclear pores we performed colocalisation experiments using antibodies against Nup189, an

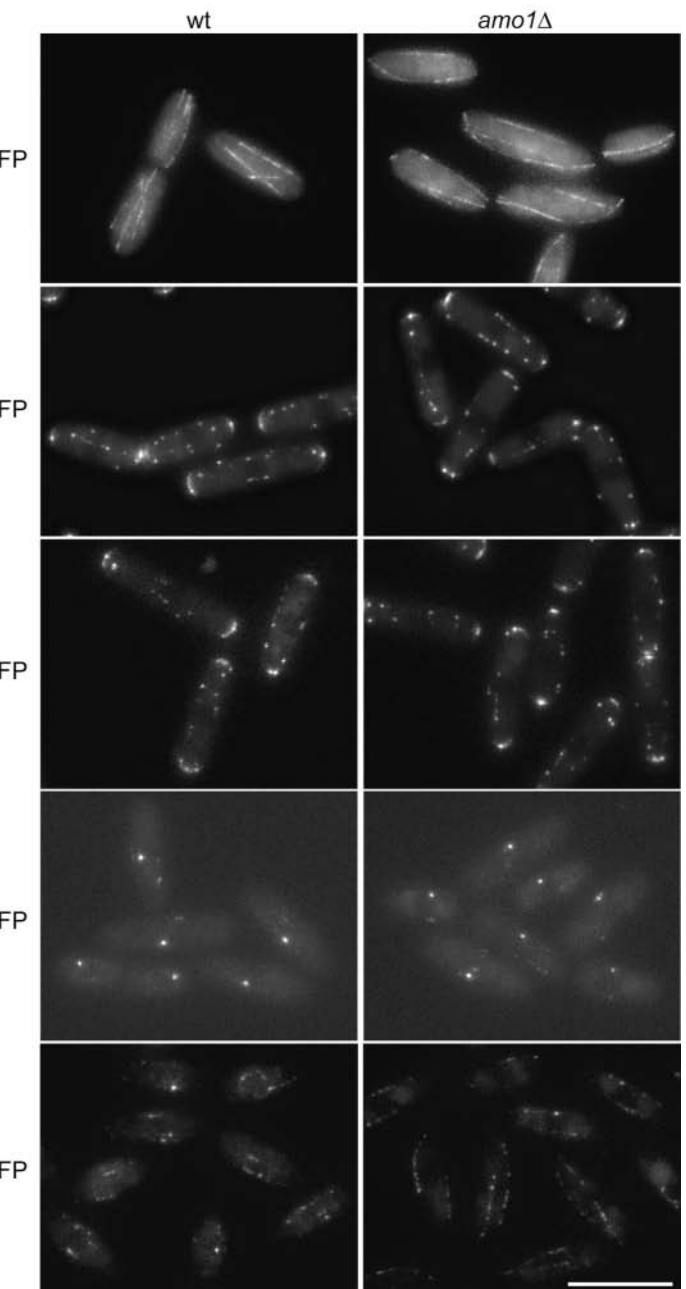


Fig. 4. Microtubule loading is not defective in *amo1Δ* cells. Localisation of Klp5-GFP on interphase microtubules, Tea2-GFP on microtubules and at cell ends, Tip1-GFP on microtubules and at cell ends, Alp4-GFP at the SPB and on microtubule satellites, and Mod20-GFP at MTOCs and microtubule satellites in live wild-type and *amo1Δ* cells. Bar, 10 μ m.

essential FG nucleoporin previously shown to localise to nuclear pores (Tange et al., 2002). Amo1-myc was detected with myc antibodies. Cells were imaged by epifluorescence microscopy in several focal planes across their entire thickness and images were deconvolved. Analysis of single focal planes through the nucleus revealed that Amo1-myc was found on the same circumference as Nup189, suggesting that Amo1-myc is localised at the nuclear membrane (Fig. 5B). Signals corresponding to Nup189 and Amo1-myc barely coincided, and in fact, when analysing a single focal plane through the middle of the nucleus, dots of Nup189

alternated with dots of Amo1. Similar results were obtained with the mAb414 antibody used as a general reagent to detect nuclear pores (data not shown). This suggests that Amo1 is not a component of the nuclear pores, but is localised at the nuclear membrane.

Despite the absence of colocalisation with nuclear pores, we asked if Amo1 was involved in nucleo-cytoplasmic transport that could indirectly lead to the microtubule defects. We tested

nuclear import by analysing the localisation of the fusion protein NLS-LacI-GFP, which in wild-type cells is targeted into the nucleus owing to the presence of the nuclear localisation sequence (NLS) signal (Fig. 5C). The fusion protein was imported into the nucleus in all *amo1Δ* cells (Fig. 5C), indicating that there is no defect in NLS-mediated protein import into the nucleus. Mid1, a protein required for the correct placement of the actin ring for cytokinesis, shuttles between the nucleus and the cell cortex in an NLS/NES (nuclear export sequence)-dependent manner in wild-type cells (Paoletti and Chang, 2000). We did not observe defects in the nuclear and cortical localisation of Mid1 in *amo1Δ* cells (data not shown), indicating that nuclear import and export of Mid1 is not affected.

Lack of some nuclear pore proteins leads to a disorganisation of the nuclear pores and mislocalisation of its components (Baï et al., 2004). Therefore, we examined the localisation of Nup189 in *amo1Δ* cells by immunofluorescence. Nup189 appeared in a dotted pattern at the nuclear periphery, similar to that observed in wild-type cells (Fig. 5D), suggesting that organisation of the nuclear pore complex is not perturbed in *amo1Δ* cells. Thus, although we cannot definitely rule out a role in nucleo-cytoplasmic transport, our results suggest that Amo1 is not required for this process.

A

Amo1	174	TSNQFNK-P-TQNSPFN--SFSNNNNSFNNN--QQAND-IFGAPTTSAFTSQLNASPFSSQ	226
Nup42	130	TSNPFKSPGSMGSAFGQPAPGANKTAIPSSSVSNNSNSAFGAASNTPLTT---TSPFG-	185
		*** * . * * : . * . * . : * . * : : . . . : * : * * : : : : * : * * : : * * : * * * .	
Amo1	227	NTSSNSPTGSNPVQNNPSSFGSSSFGSATSGPSAFGGISQPNSSFVNSGQGI-PNSSFSS	285
Nup42	186	SLQQN--ASQN-ASSTSSAFGKPTFGAATNTQSPFGTI-Q-NTS-TSSGTGVSPFGTFGT	239
		. . . * . . . * * : * * : * * * : * * * * * * * * * * * * * * * * * * : * : * : * .	
Amo1	286	FSQVASGFSSQSN-VNDPSSI FGP TVASGFGIQNPQQSAFQNLNTQFSLPNNSQPVFGH	344
Nup42	240	NSNNKSPFSSNLQSGAGAGSSPFG-TTTSKANNNNNVGSSAFGTTNNQSPFSGGSGGTFGS	298
		* : * * * : * . . . * * * * * : * : * : * * * . * * * . * * .	
Amo1	345	TS-LTQPVNPNQ-FTV--QPPATFMQQPQGP--VP-PNTTPEPFFANVTSKISASGFS	396
Nup42	299	ASNLNK--NTNGNFQSSFGNKGFSFGITPQNDANKVQSQNSPFGQTMPTDNPINSLK--S	354
		* * * : * * * * * : * : * * * . * . * : * * * . . : * * * . *	
Amo1	397	NDNPANKNIIQTPMFGS---SNTIDGPINPI-GASSIQTLDDQVEMSNQNLAPFPEMI	452
Nup42	355	NGNATSPFGQQMNTNWNANTATGKIRFVQGLSSEK--DGILELAD---LA--EETL	406
		* . * : . . : * * * : : * * * * . : * * * : * . : * : : * * * * * * * * .	
Amo1	453	QQFEAQDFIPGKVPTTAPPPQFC-	475
Nup42	407	KIFRANKFELGLVPDIPPPPALVA	430
		: * . * : * * * * * * * * .	

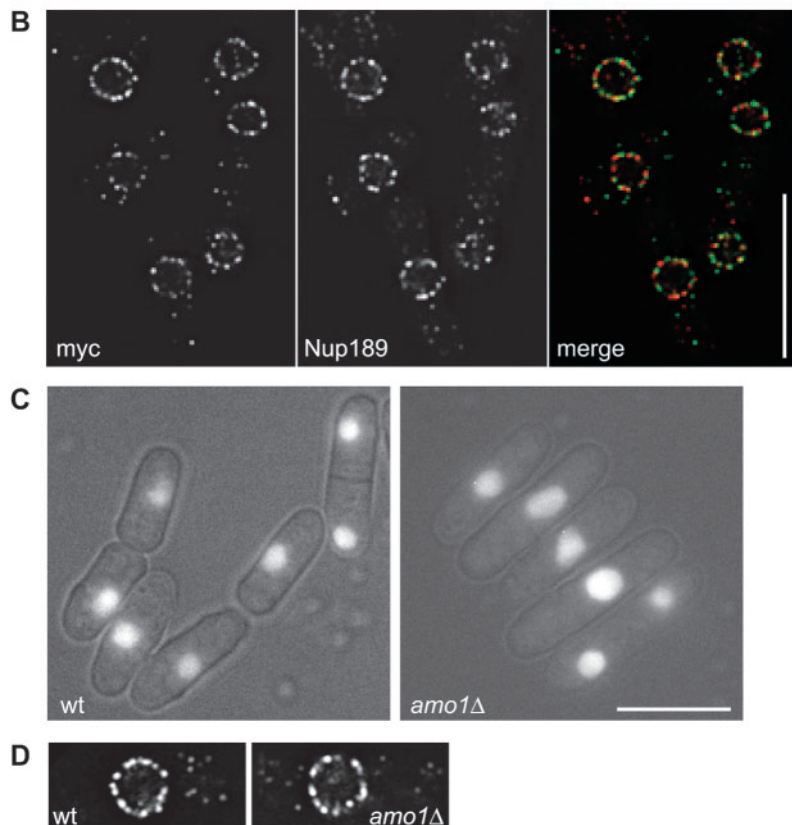


Fig. 5. *Amo1Δ* cells are not defective in NPC organisation. (A) Alignment of *S. pombe* Amo1 and *S. cerevisiae* Nup42 sequences, showing conservation of some FG repeats (in red). Protein alignment was carried out with CLUSTALW. (B) Immunofluorescence of cells expressing Amo1-myc with anti-myc (green) and anti-Nup189 (red) antibodies. (C) NLS-LacI-GFP localisation in live wild-type and *amo1Δ* cells. (D) Nup189 immunofluorescence in wild-type and *amo1Δ* cells. Bar, 10 μm.

Discussion

To gain better understanding of the regulation of microtubule organisation and dynamics, we performed an overexpression screen, and identified 39 genes whose overexpression leads to microtubule defects. At the induction levels used, in most cases only interphase abnormalities were observed; a few genes caused both interphase and spindle defects, or only mitotic defects. Six of the identified genes had been previously reported to affect microtubule function or mitosis, confirming that the screen was working. The genes identified were classified into several functional groups, based on reported function, protein sequence homology and protein domains. Seven genes did not show any sequence homology or identifiable protein domains and were classified as orphans. There is no correlation between these functional categories and the overexpression phenotypes observed. As a secondary screen to identify those genes that have a direct effect on microtubule regulation, we deleted all of the unknown or uncharacterised genes identified, and looked for microtubule defects in the deleted strains. We tested the viable haploid deleted strains for growth and morphology, sensitivity to microtubule poisons and microtubule organisation, and analysed the lethal deletions by immunofluorescence in spore germination assays. Fifteen haploid viable deletions showed a phenotype in at least one of the assays, with two of them displaying a phenotype in all three assays,

suggesting that they are indeed involved in microtubule function. Again in this case we could observe no correlation between functional category and deletion phenotype. The rest of the viable deletions (13/28) behaved just like wild-type cells in all the conditions tested. There are several explanations for this. Redundant genes might be present that undertake the function of the genes deleted. Alternatively, the overexpression might cause a microtubule defect by titration of a different protein required for proper microtubule organisation. Finally, the microtubule defect caused by overexpression might be the consequence of a more general disruption of cellular activities. Six of the deletions were lethal; they included three genes involved in vesicle traffic, two genes involved in nuclear function and one encoding a microtubule-associated protein that is also required for ribosome biogenesis, in agreement with the importance of these processes for viability.

Amo1 was identified as a gene whose overexpression leads to bundling of microtubules on one side of the cell. Cells lacking *amo1* also have aberrant microtubules, confirming that *amo1* is involved in microtubule organisation. Microtubule bundles in *amo1Δ* cells are less abundant, are thicker and curl around cell ends. We have determined that *amo1Δ* microtubules spend longer at the cell tip than the wild type, and that they grow in a less coordinated fashion, with more than one microtubule in a bundle touching the cell tip at the same time observed more often than in wild-type cells.

Amo1 localises in dots at the nuclear periphery, in a pattern reminiscent of nuclear pore complex (NPC) proteins. Similarity searches identified Nup42 from *S. cerevisiae*, a nucleoporin required for mRNA export from the nucleus (Vainberg et al., 2000), as the closest homologue. However, the similarity is mainly based in the presence of a few FG repeats. Nup42 has a closer homologue in *S. pombe*, the nucleoporin Nup189, which contains a higher number and conservation of the FG repeats. FG repeats appear in extensive regions in the FG family of nucleoporins, and are thought to facilitate the passage of transporter-cargo complexes through the nuclear pore by binding to karyopherins (Fahrenkrog and Aebi, 2003). The FG nucleoporins exist in a disordered state, with biochemical properties similar to natively unfolded proteins (Denning et al., 2003). This unordered structure has biochemical features that allow a variety of interactions with different partners with fast association-dissociation rates. Like FG nucleoporins, Amo1 is enriched in charged and polar amino acids, which suggests that it could also exist in an unfolded state. It is possible that Amo1 forms flexible 'arms' anchored in the nuclear membrane that can provide transient interactions with other molecules or polymers such as microtubules. These interactions could be important for nuclear positioning, which relies on MT pushing on the nuclear membrane (Tran et al., 2001), and in fact lack of Amo1 causes a nuclear positioning defect. Nup42 localises to the cytoplasmic side of the NPC (Rout et al., 2000), and it would be interesting to determine if Amo1 is asymmetrically localised to the cytoplasmic face of the nuclear envelope.

Despite the similarity with nucleoporins, we do not believe Amo1 affects NPC translocation function. First, Amo1 does not precisely colocalise with the *S. pombe* nucleoporin Nup189, a known component of nuclear pores (Tange et al., 2002), and it is likely that Amo1 and Nup189 exclude each other. Second, lack of Amo1 does not seem to affect NPC distribution or import of a marker protein into the nucleus. Amo1 is not required for

import or export of Mid1 from the nucleus either. This suggests that the microtubule defect of *amo1Δ* cells is not an indirect consequence of a general failure in nucleo-cytoplasmic trafficking. Mutations in several nucleoporins lead to other nuclear defects namely aberrant nuclear envelope shape, nucleolar structure or spindles, phenotypes thought to arise from a defective nucleo-cytoplasmic transport (Shan et al., 1997). These defects are not observed in *amo1Δ* cells. However, we cannot completely exclude some other kind of defect like export of RNAs or an altered rate of protein import/export.

It is difficult to reconcile the nuclear surface localisation of Amo1 with its effect on microtubule dwelling time at cell tips. Microtubule loading of factors affecting microtubule dynamics seemed the obvious link, as it usually takes place in the vicinity of the nucleus (Behrens and Nurse, 2002; Browning et al., 2003; Busch et al., 2004). However, we have been unable to detect a defect in microtubule loading of several of these proteins, in particular the obvious candidates whose absence gives a similar phenotype to the lack of Amo1. It is possible that such a factor is still unidentified. It could be a destabilising factor or a protein that promotes catastrophe when the microtubule reaches the tip, for instance by unloading a stabilising microtubule-associated protein. The possibility also remains that Amo1 itself is localised on microtubules from where it regulates their dynamics, and that we have so far been unable to detect this location.

We have shown that the lack of Amo1 has an effect on the coordination of microtubules growing from the overlap region in the middle of the cell to the cell tip. In contrast to wild-type cells, where microtubules in a given bundle seem to reach the cell tip one at a time (Sagolla et al., 2003), in *amo1Δ* cells there is often more than one microtubule in the same bundle touching the cell tip at any one time. This results in longer cell tip contact of the microtubule bundle, which can lead to microtubules curling round cell ends when bundles on both sides of the cell are touching the tip. Microtubule bundles also contact the nuclear membrane (Tran et al., 2001), and therefore Amo1 at this localisation could be involved in regulating the growth of individual microtubules in coordination with their bundle partners. For instance, lack of pushing at the nuclear envelope contact site when a microtubule depolymerises from the cell tip might signal another microtubule to grow. Several nucleoporins localise to kinetochores and have been reported to have a specific role in chromosome segregation and checkpoint control (Belgareh et al., 2001; Kerscher et al., 2001; Iouk et al., 2002; Chen et al., 2004), where a similar interaction with microtubules could take place. Indeed, microtubule attachment to the nuclear envelope does not seem to be impaired by *amo1* deletion, as we observed typical nuclear membrane deformations produced when microtubules attached to the nucleus grow against the cell tips in cells lacking Amo1 (Tran et al., 2001).

Amo1 seems to cooperate with Tea1 in the maintenance of cell polarity by regulating the proper dynamics of microtubules, and Tea1 localisation is mildly affected by Amo1. This is possibly due to the fact that microtubules in cells lacking Amo1 hit the cortex repeatedly in a few positions, where Tea1 then accumulates, instead of throughout the entire tip. This could have an effect on morphology causing cells to bend. Amo1 is also required for NETO as *amo1Δ* grows mainly in a monopolar fashion. However, *amo1Δ* cells have the ability to recognise both cell ends and to use them as sites for growth, as NETO can be induced either by increasing the pool of free monomeric actin or

by increasing cell length (unpublished observations). It is therefore not likely that the abnormal localisation of Tea1 is the cause of the NETO defect, because a Lat A pulse of *tea1Δ* cells leads mainly to delocalised actin patches and cells do not become bipolar (Rupes et al., 1999).

In conclusion, we have identified a gene, *amol1*, encoding a novel protein that is required for the correct coordination of microtubule growth and cell end termination. The nuclear rim localisation of Amol1 suggests that an interaction between microtubules and nucleus is important for proper microtubule behaviour.

We thank S. Castagnetti, J. Hayles and R. Carazo-Salas for critical reading of the manuscript. We also thank I. Hagan, K. Sawin and R. Tsien for providing strains, antibodies and mRFP1 (monomeric red fluorescent protein). We specially thank M. Godinho-Ferreira and R. Carazo-Salas for their help in the last stages of this work. M.P. was funded by Cancer Research UK.

References

- Arellano, M., Niccoli, T. and Nurse, P. (2002). Tea3p is a cell end marker activating polarized growth in *Schizosaccharomyces pombe*. *Curr. Biol.* **12**, 751-756.
- Bahler, J., Wu, J. Q., Longtine, M. S., Shah, N. G., McKenzie, A. 3rd, Steever, A. B., Wach, A., Philippsen, P. and Pringle, J. R. (1998). Heterologous modules for efficient and versatile PCR-based gene targeting in *Schizosaccharomyces pombe*. *Yeast* **14**, 943-951.
- Bai, S. W., Rouquette, J., Umeda, M., Faigle, W., Loew, D., Sazer, S. and Doye, V. (2004). The fission yeast Nup107-120 complex functionally interacts with the small GTPase Ran/Spi1 and is required for mRNA export, nuclear pore distribution, and proper cell division. *Mol. Cell Biol.* **24**, 6379-6392.
- Behrens, R. and Nurse, P. (2002). Roles of fission yeast tea1p in the localization of polarity factors and in organizing the microtubular cytoskeleton. *J. Cell Biol.* **157**, 783-793.
- Belgareh, N., Rabut, G., Bai, S. W., van Overbeek, M., Beaudouin, J., Daigle, N., Zatschina, O. V., Pasteau, F., Labas, V., Fromont-Racine, M., Ellenberg, J. and Doye, V. (2001). An evolutionarily conserved NPC subcomplex, which redistributes in part to kinetochores in mammalian cells. *J. Cell Biol.* **154**, 1147-1160.
- Browning, H., Hayles, J., Mata, J., Aveline, L., Nurse, P. and McIntosh, J. R. (2000). Tea2p is a kinesin-like protein requires to generate polarized growth in fission yeast. *J. Cell Biol.* **151**, 15-27.
- Browning, H., Hackney, D. D. and Nurse, P. (2003). Targeted movement of cell end factors in fission yeast. *Nat. Cell Biol.* **5**, 812-818.
- Brunner, D. and Nurse, P. (2000). CLIP170-like tip1p spatially organizes microtubular dynamics in fission yeast. *Cell* **102**, 695-704.
- Busch, K. E., Hayles, J., Nurse, P. and Brunner, D. (2004). Tea2p kinesin is involved in spatial microtubule organization by transporting tip1p on microtubules. *Dev. Cell* **6**, 831-843.
- Campbell, R. E., Tour, O., Palmer, A. E., Steinbach, P. A., Baird, G. S., Zacharias, D. A. and Tsien, R. Y. (2002). A monomeric red fluorescent protein. *Proc. Natl Acad. Sci. USA* **99**, 7877-7882.
- Chen, X. Q., Du, X., Liu, J., Balasubramanian, M. K. and Balasubramanian, D. (2004). Identification of genes encoding putative nucleoporins and transport factors in the fission yeast *Schizosaccharomyces pombe*: a deletion analysis. *Yeast* **21**, 495-509.
- Denning, D. P., Patel, S. S., Uversky, V., Fink, A. L. and Rexach, M. (2003). Disorder in the nuclear pore complex: The FG repeat regions of nucleoporins are natively unfolded. *Proc. Natl Acad. Sci. USA* **100**, 2450-2455.
- Ding, D.-Q., Chikashige, Y., Haraguchi, T. and Hiraoka, Y. (1998). Oscillatory nuclear movement in fission yeast meiotic prophase is driven by astral microtubules, as revealed by continuous observation of chromosomes for normal nuclear segregation in yeast. *Proc. Natl Acad. Sci. USA* **90**, 11172-11176.
- Drummond, D. R. and Cross, R. A. (2000). Dynamics of interphase microtubules in *Schizosaccharomyces pombe*. *Curr. Biol.* **10**, 766-775.
- Fahrenkrog, B. and Aebi, U. (2003). The nuclear pore complex: nucleocytoplasmic transport and beyond. *Nat. Rev. Mol. Cell Biol.* **4**, 757-766.
- Feierbach, B., Verde, F. and Chang, F. (2004). Regulation of a formin complex by the microtubule plus end protein tea1p. *J. Cell Biol.* **165**, 697-707.
- Hagan, I. M. (1998). The fission yeast microtubule cytoskeleton. *J. Cell Sci.* **111**, 1603-1612.
- Hagan, I. M. and Yanagida, M. (1995). The product of the spindle formation gene *sad1+* associates with the fission yeast spindle pole body and is essential for viability. *J. Cell Biol.* **129**, 1033-1047.
- Iouk, T., Kerscher, O., Scott, R. J., Basrai, M. A. and Wozniak, R. W. (2002). The yeast nuclear pore complex functionally interacts with components of the spindle assembly checkpoint. *J. Cell Biol.* **159**, 807-819.
- Kerscher, O., Hieter, P., Winey, M. and Basrai, M. A. (2001). Novel role for a *Saccharomyces cerevisiae* nucleoporin, Nup170p, in chromosome segregation. *Genetics* **157**, 1543-1553.
- Mata, J. and Nurse, P. (1997). Tea1 and the microtubular cytoskeleton are important for generating global spatial order within the fission yeast cell. *Cell* **89**, 939-949.
- Mitchison, J. M. and Nurse, P. (1985). Growth in cell length in the fission yeast *Schizosaccharomyces pombe*. *J. Cell Sci.* **75**, 357-376.
- Moreno, S., Klar, A. and Nurse, P. (1991). Molecular genetic analysis of fission yeast *Schizosaccharomyces pombe*. *Methods Enzymol.* **194**, 795-823.
- Niccoli, T., Arellano, M. and Nurse, P. (2003). Role of Tea1p, Tea3p and Pom1p in the determination of cell ends in *Schizosaccharomyces pombe*. *Yeast* **20**, 1349-1358.
- Paoletti, A. and Chang, F. (2000). Analysis of mid1p, a protein required for placement of the cell division site, reveals a link between the nucleus and the cell surface in fission yeast. *Mol. Biol. Cell* **11**, 2757-2773.
- Rout, M. P., Aitchison, J. D., Suprpto, A., Hjertaas, K., Zhao, Y., and Chait, B. T. (2000). The Yeast Nuclear Pore Complex. Composition, architecture, and transport mechanism. *J. Cell Biol.* **148**, 635-652.
- Rupes, I., Zhengping, J. and Young, P. G. (1999). Ssp1 promotes actin depolymerization and is involved in stress response and new end take-off control in fission yeast. *Mol. Biol. Cell* **10**, 1495-1510.
- Russell, P. (1989). Gene cloning and expression in fission yeast. In *Molecular Biology of the Fission Yeast* (ed. A. Nasim, P. Young and B. F. Johnson), pp. 244-272. San Diego, CA: Academic Press.
- Sagolla, M. J., Uzawa, S. and Cande, W. Z. (2003). Individual microtubule dynamics contribute to the function of mitotic and cytoplasmic arrays in fission yeast. *J. Cell Sci.* **116**, 4891-4903.
- Sawin, K. E., Lourenco, P. C. and Snaith, H. (2004). Microtubule nucleation at non-spindle pole body microtubule-organizing centers requires fission yeast centrosomin-related protein mod20p. *Curr. Biol.* **14**, 763-775.
- Shan, X., Xue, Z., Euskirchen, G. and Melese, T. (1997). NNF1 is an essential yeast gene required for proper spindle orientation, nucleolar and nuclear envelope structure and mRNA export. *J. Cell Sci.* **110**, 1615-1624.
- Snaith, H. A. and Sawin, K. E. (2003). Fission yeast mod5p regulates polarized growth through anchoring of tea1p at cell tips. *Nature* **423**, 647-651.
- Strawn, L. A., Shen, T., Shulga, N., Goldfarb, D. S. and Wente, S. R. (2004). Minimal nuclear pore complexes define FG repeat domains essential for transport. *Nat. Cell Biol.* **6**, 197-206.
- Tange, Y., Hirata, A. and Niwa, O. (2002). An evolutionarily conserved fission yeast protein, Ned1, implicated in normal nuclear morphology and chromosome stability, interacts with Dis3, Pim1/RCC1 and an essential nucleoporin. *J. Cell Sci.* **115**, 4375-4385.
- Tran, P. T., Marsh, L., Doye, V., Inoue, S. and Chang, F. (2001). A mechanism for nuclear positioning in fission yeast based on microtubule pushing. *J. Cell Biol.* **153**, 397-411.
- Vainberg, I. E., Dower, K. and Rosbash, M. (2000). Nuclear export of heat shock and non-heat-shock mRNA occurs via similar pathways. *Mol. Cell Biol.* **20**, 3996-4005.
- Venkatram, S., Tasto, J. J., Feoktistova, A., Jennings, J. L., Link, A. J. and Gould, K. L. (2004). Identification and characterization of two novel proteins affecting fission yeast gamma-tubulin complex function. *Mol. Cell Biol.* **15**, 2287-2301.
- West, R. R., Vaisberg, E. V., Ding, R., Nurse, P. and McIntosh, J. R. (1998). *cut11(+)*: A gene required for cell cycle-dependent spindle pole body anchoring in the nuclear envelope and bipolar spindle formation in *Schizosaccharomyces pombe*. *Mol. Biol. Cell* **9**, 2839-2855.
- West, R. R., Malmstrom, T., Troxell, C. L. and McIntosh, J. R. (2001). Two related kinesins, klp5+ and klp6+, foster microtubule disassembly and are required for meiosis in fission yeast. *Mol. Biol. Cell* **12**, 3919-3932.
- Zimmerman, S., Tran, P. T., Daga, R. R., Niwa, O. and Chang, F. (2004). Rsp1, a J domain protein required for disassembly and assembly of microtubule organizing centers during the fission yeast cell cycle. *Dev. Cell* **6**, 497-509.